



Supplement of

Eddy-covariance fluxes of CO₂, CH₄ and N₂O in a drained peatland forest after clear-cutting

Olli-Pekka Tikkasalo et al.

Correspondence to: Olli-Pekka Tikkasalo (olli-pekka.tikkasalo@luke.fi)

The copyright of individual parts of the supplement might differ from the article licence.

Table S1. Comparison of model performance measured with expected log posterior density leave-one-out cross-validation (ELPD-LOO). The model exhibiting the highest ELPD-LOO was selected for subsequent analysis and is presented in bold for both the CH₄ and N₂O flux.

Model	Number of parameters	ELPD-LOO	Model rank
CH₄			
Simple	3	2585.6	22
Simple θ	4	3206.4	11
Full ST3	9	2748.6	16
Full ST4	11	2771.4	15
Full ST5	13	2772.4	14
Full ST6	15	2804.5	12
Full ST9	21	2801.6	13
Full no δ ST3	6	2669.0	21
Full no δ ST4	7	2677.1	20
Full no δ ST5	8	2691.8	19
Full no δ ST6	9	2704.0	17
Full no δ ST9	12	2702.3	18
Full θ ST3	10	3414.5	7
Full θ ST4	12	3468.7	4
Full θ ST5	14	3483.7	3
Full θ ST6	16	3526.3	2
Full θ ST9	22	3529.5	1
Full θ no δ ST3	7	3340.2	10
Full θ no δ ST4	8	3375.0	9
Full θ no δ ST5	9	3408.4	8
Full θ no δ ST6	10	3428.7	6
Full θ no δ ST9	13	3435.5	5
N₂O			
Simple	3	-3751.6	22
Simple θ	4	-3714.6	21
Full ST3	9	-3062.8	18
Full ST4	11	-3056.2	17
Full ST5	13	-2759.2	10
Full ST6	15	-2751.3	9
Full ST9	21	-2702.3	7
Full no δ ST3	6	-3075.1	20
Full no δ ST4	7	-3068.7	19
Full no δ ST5	8	-2775.2	12
Full no δ ST6	9	-2768.3	11
Full no δ ST9	12	-2717.8	8
Full θ ST3	10	-2917.5	15
Full θ ST4	12	-2906.2	13
Full θ ST5	14	-2537.8	4
Full θ ST6	16	-2528.7	3
Full θ ST9	22	-2452.5	1
Full θ no δ ST3	7	-2923.9	16
Full θ no δ ST4	8	-2923.9	14
Full θ no δ ST5	9	-2545.5	6

Full θ no δ ST6	10	-2537.5	5	
Full θ no δ ST9	13	-2459.8	2	

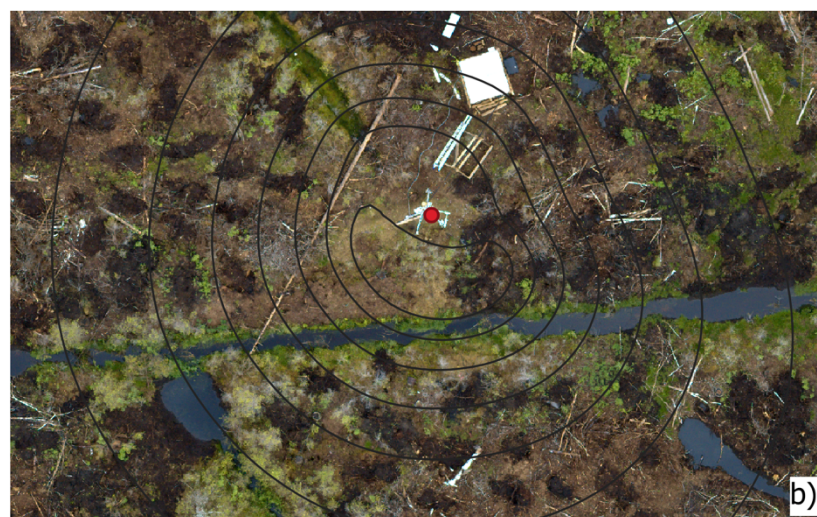
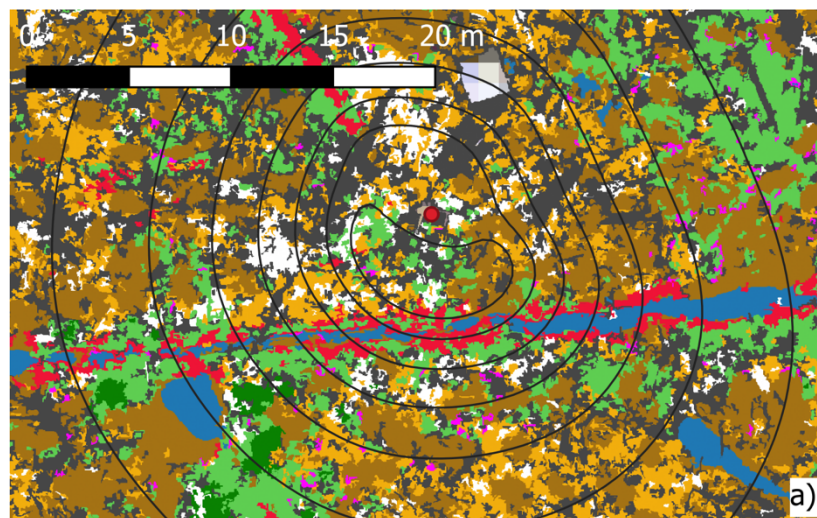


Figure S1. Close-up of surface-type classification (a) and aerial view (b) around the eddy covariance tower.

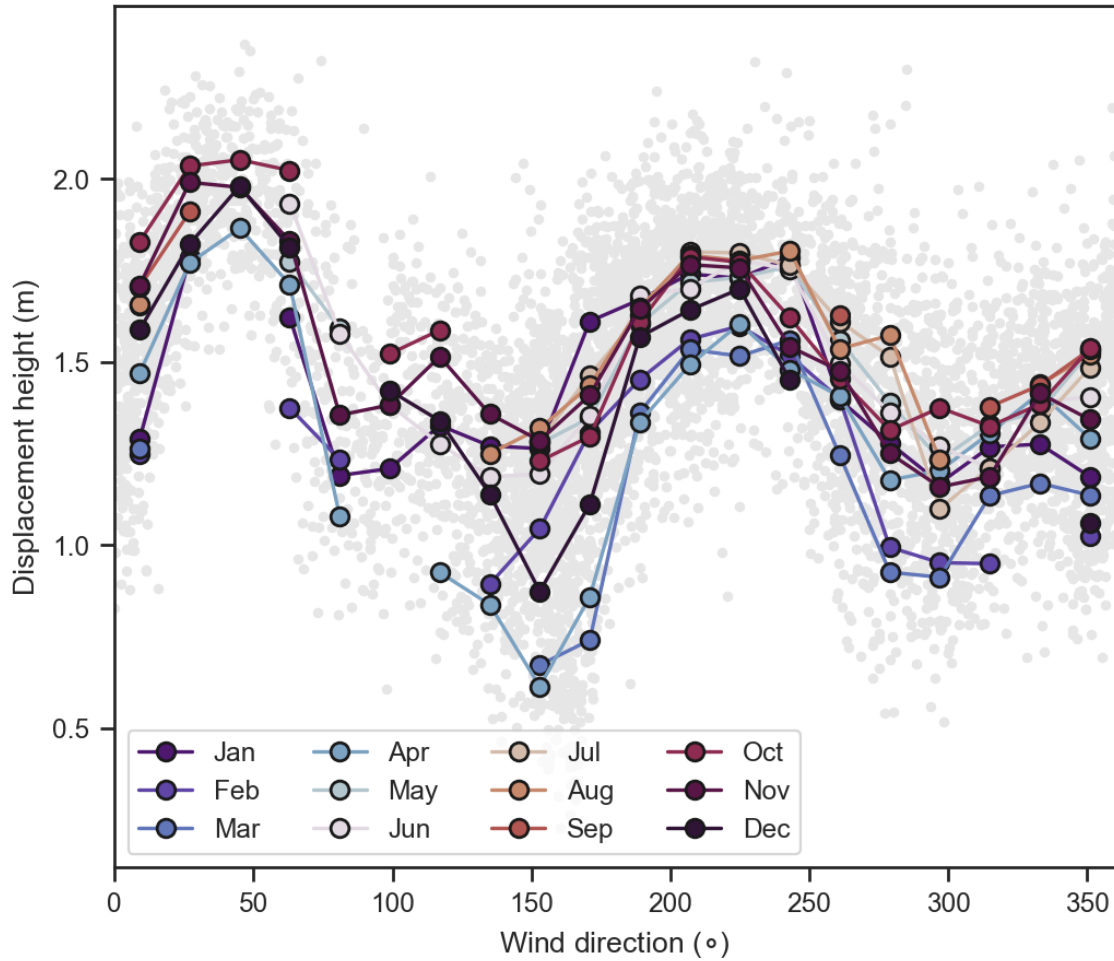


Figure S2. Displacement height at different wind directions. Grey markers shows the estimated displacement height (see Sect 2.4 in the main text) at different wind directions. Solid lines with circle markers shows the 30-day displacement height bins for each month that were used in the footprint calculations.

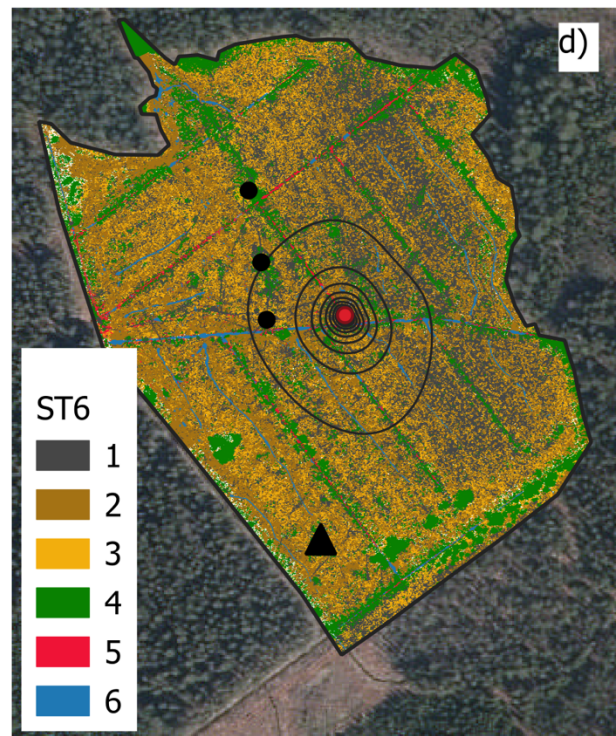
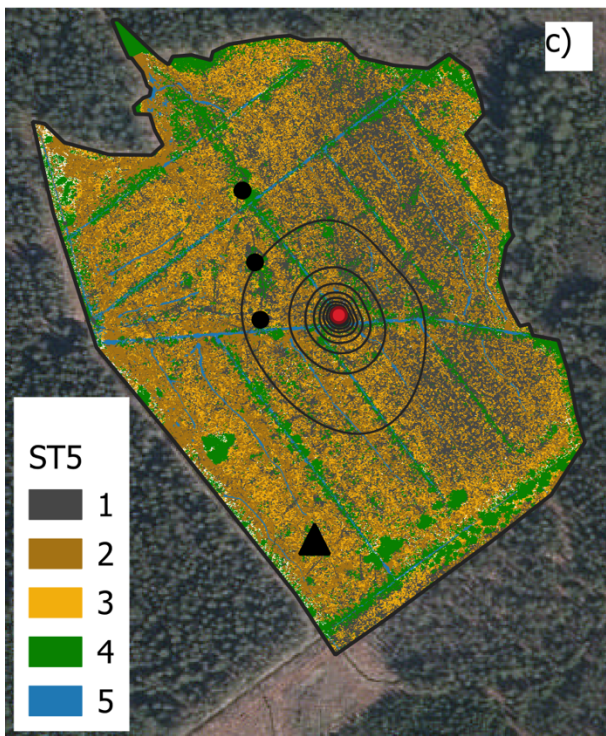
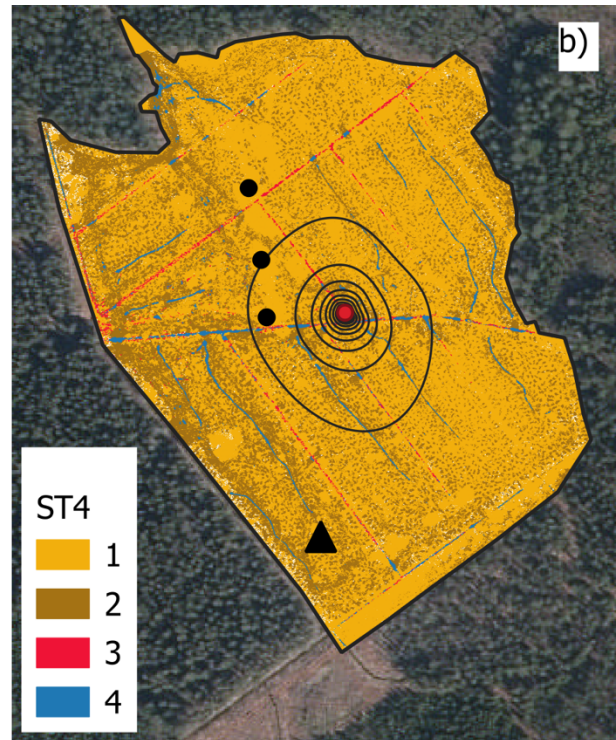
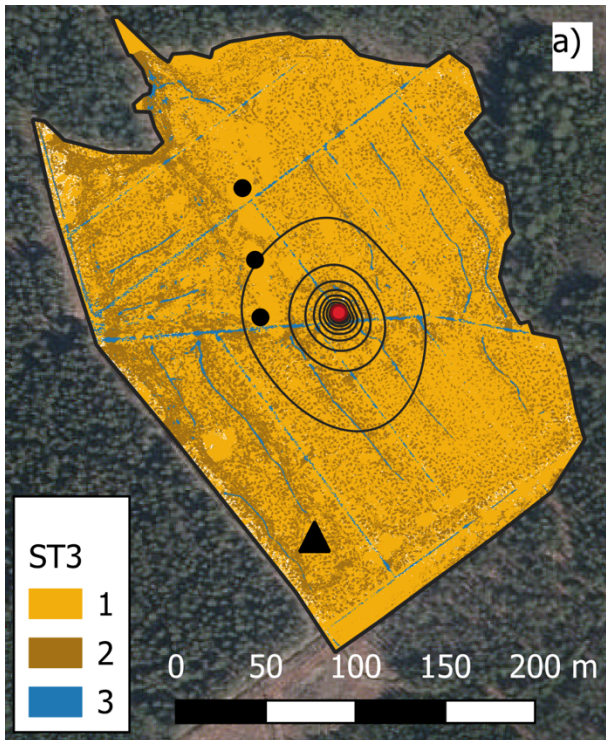


Figure S3: Surface-type classification for the clearcut area. The surface-type classification is shown for ST3 (a), ST4 (b), ST5(c) and ST6 (d). The surface-type combinations can be found from Table 2 in the main text. The background aerial photo in a-d is acquired from the National Land Survey of Finland Topographic Database (distributed with CC-BY 4.0 license, retrieved 06/2024).

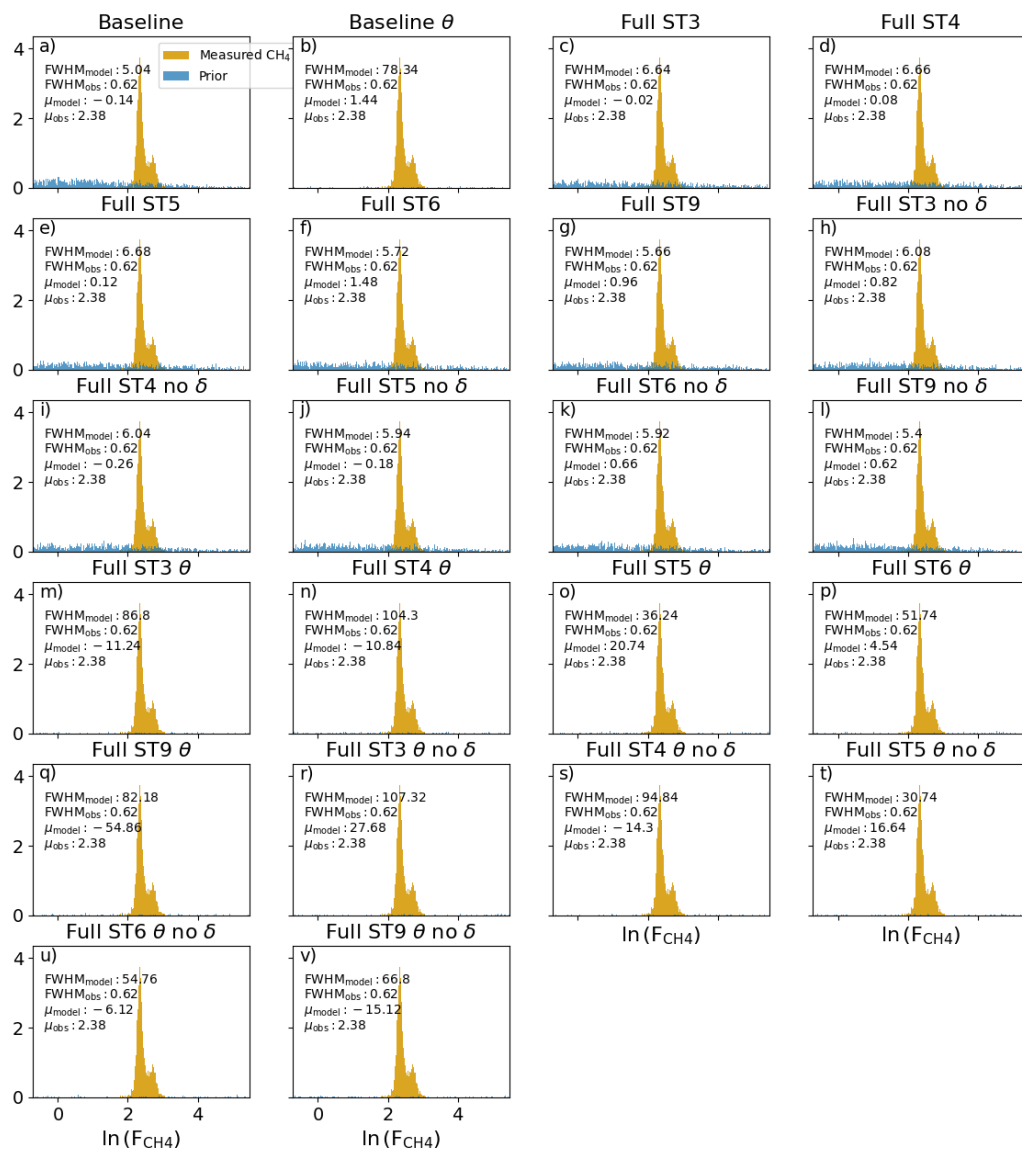


Figure S4. Prior predictive distribution and measured distribution of CH_4 at the Ränskälänkorpi study site. Different subfigures are for different models described in the main text. Each subfigure shows the full width at half maximum (FWHM) and mean value of the prior predictive and measured distribution.

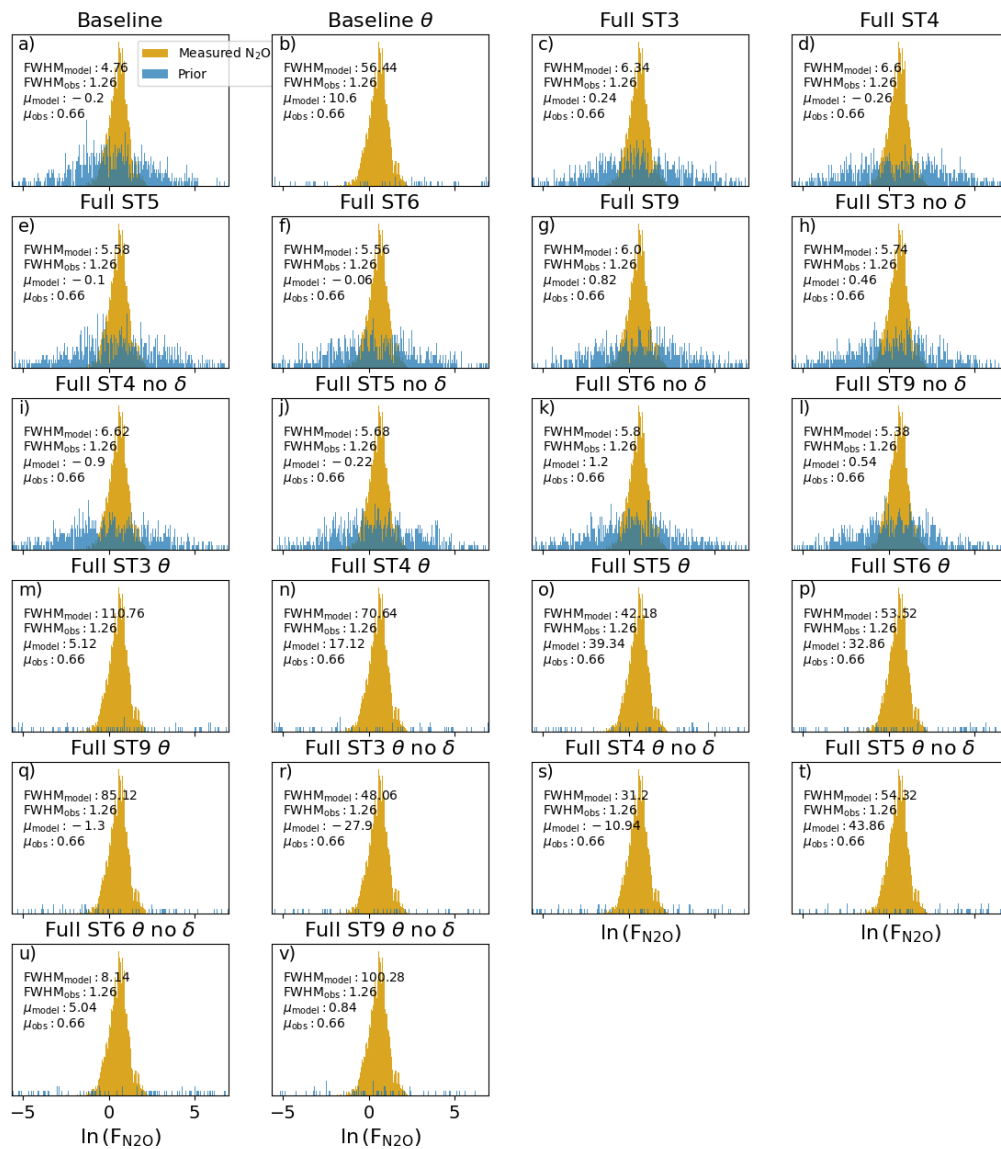


Figure S5. Prior predictive distribution and measured distribution of N_2O at the Ränskälänkorpi study site. Different subfigures are for different models described in the main text. Each subfigure shows the full width at half maximum (FWHM) and mean value of the prior predictive and measured distribution.

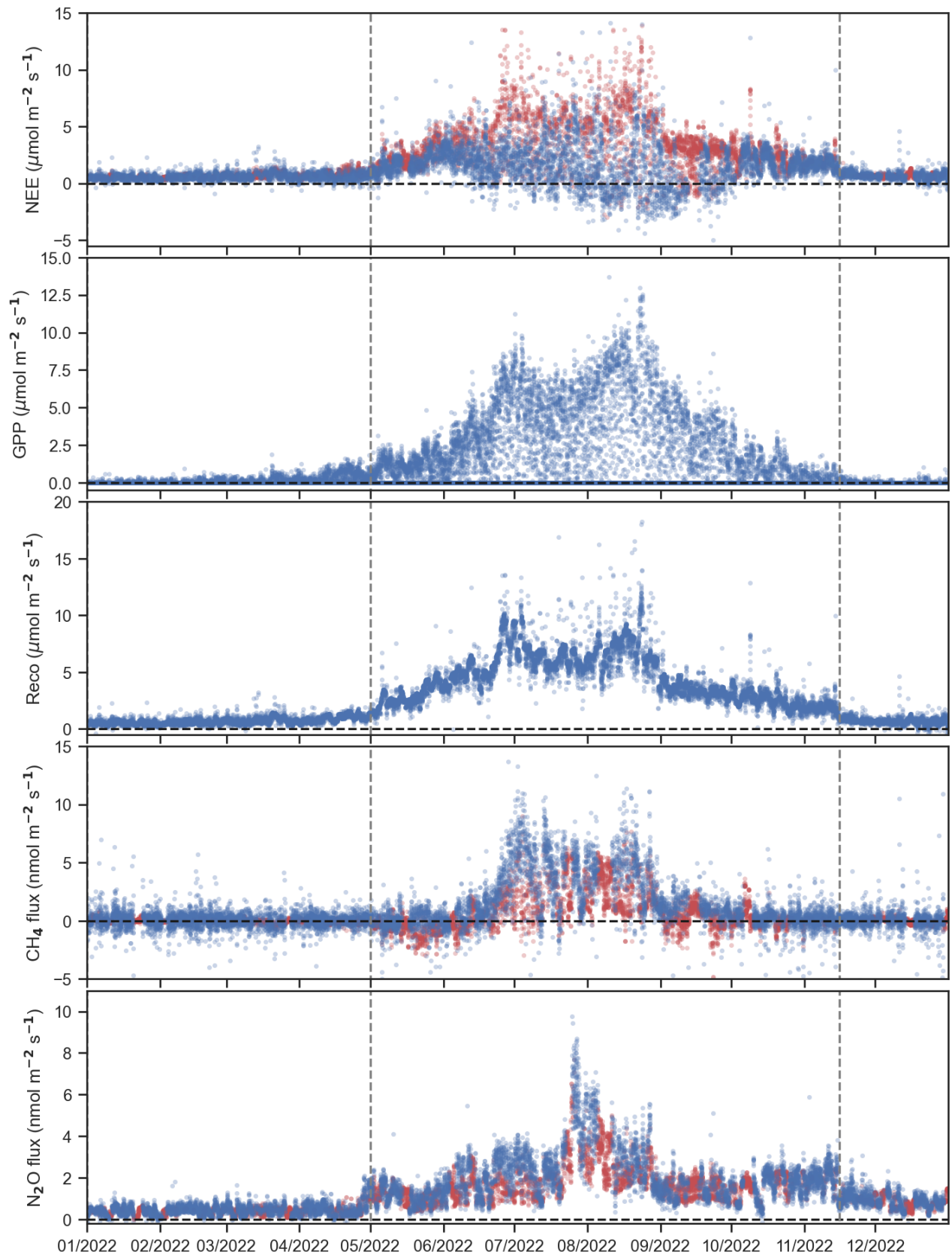


Figure S6. Time series of 30 min fluxes during the year 2022. Red symbols show gapfilled values and blue show measured values.

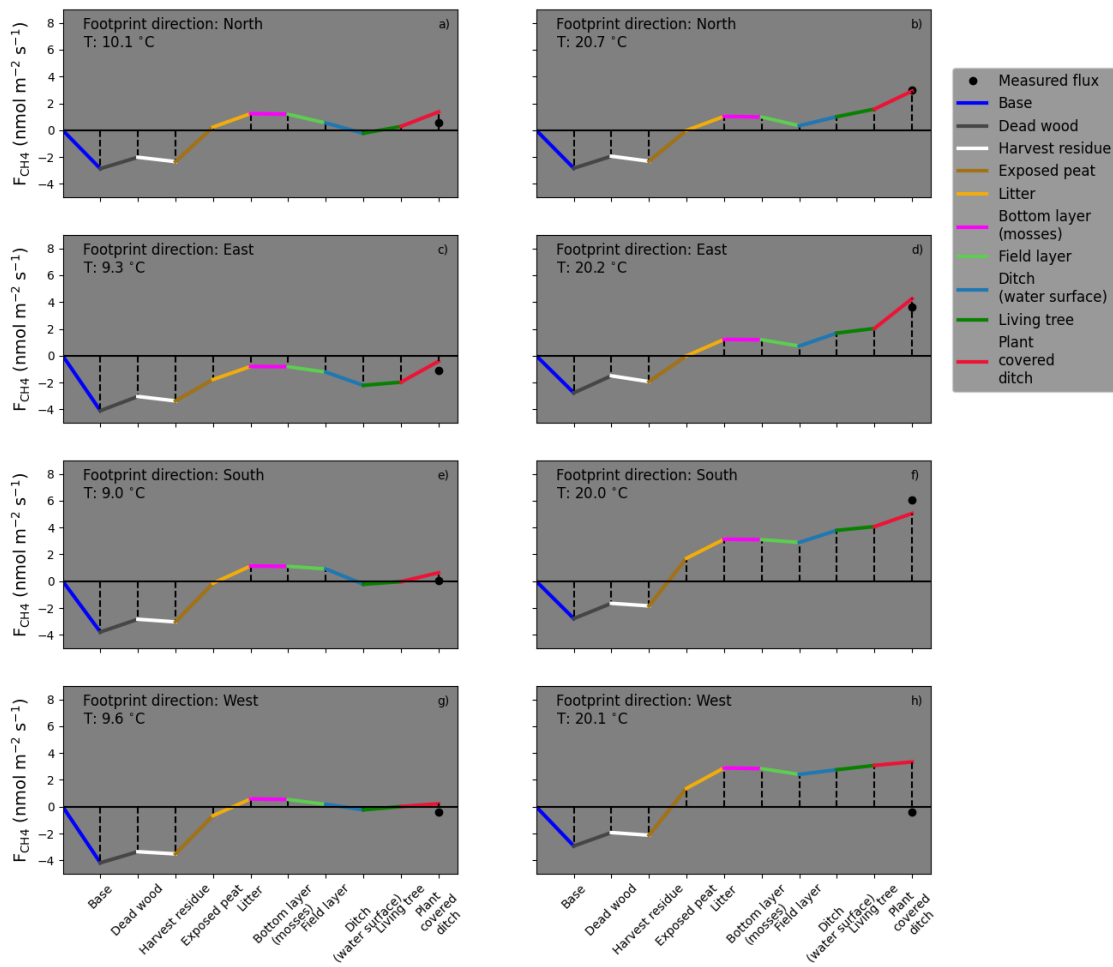


Figure S7. Contribution of each surface type to the estimated flux value in the best CH₄ model. Different subfigures show different footprint directions in the clearcut (see Fig. 1 in the main text) and the left column is for the measurement whose air temperature is closest to 283.15 K (=10°C) and right for the air temperature 293.15 K (=20°C). In each subfigure, surface types are added to the model from left to right. Base model is the baseline model as defined by Eq. (4) in the main text. Black circle shows the value of the measured flux and the final model estimate is found on the last surface type (Field layer and trees) on the horizontal axis.

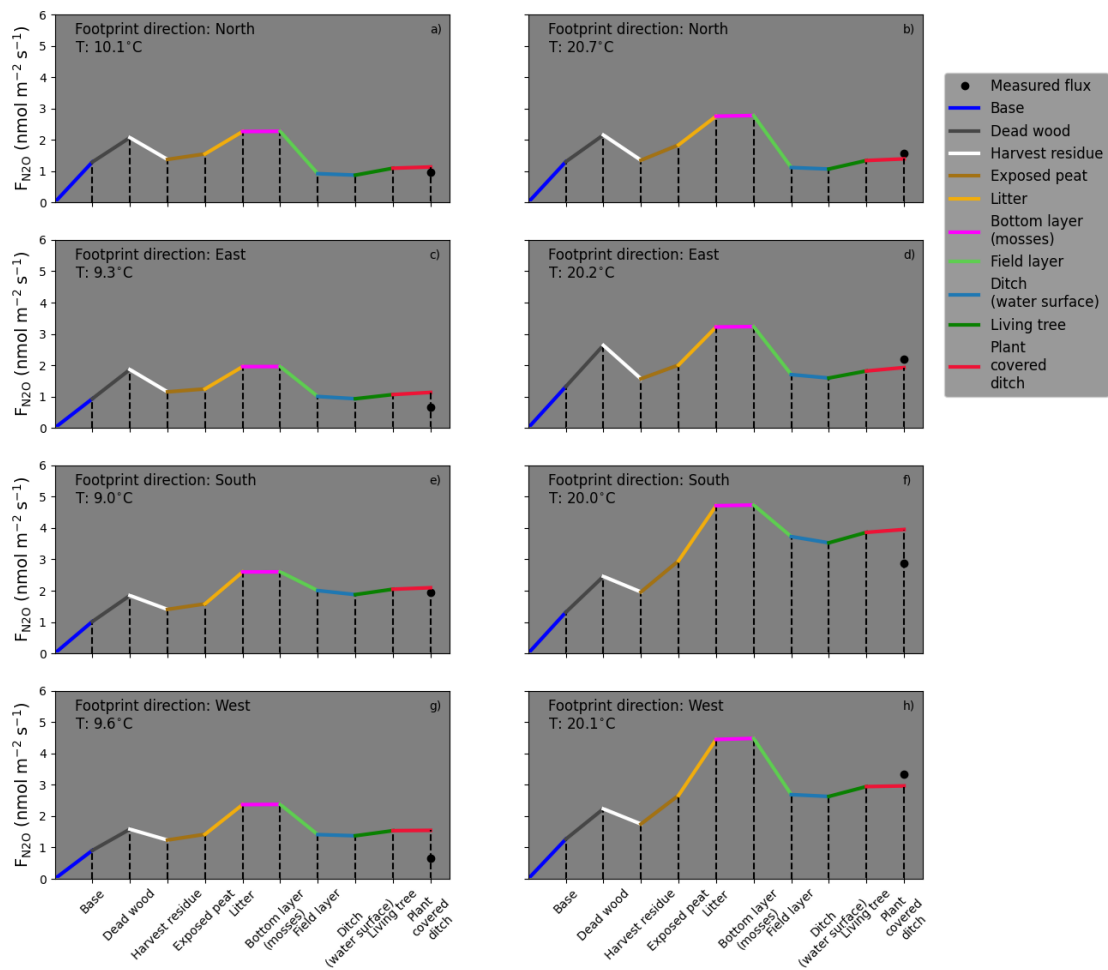


Figure S8. Contribution of each surface type to the estimated flux value in the best N_2O model. Different subfigures show different footprint directions in the clearcut (see Fig. 1 in the main text) and the left column is for the measurement whose air temperature is closest to 283.15 K (=10°C) and right for the air temperature 293.15 K (=20°C). In each subfigure, surface types are added to the model from left to right. Base model is the baseline model as defined by Eq. (4) in the main text. Black circle shows the value of the measured flux and the final model estimate is found on the last surface type (Plant covered ditch) on the horizontal axis.

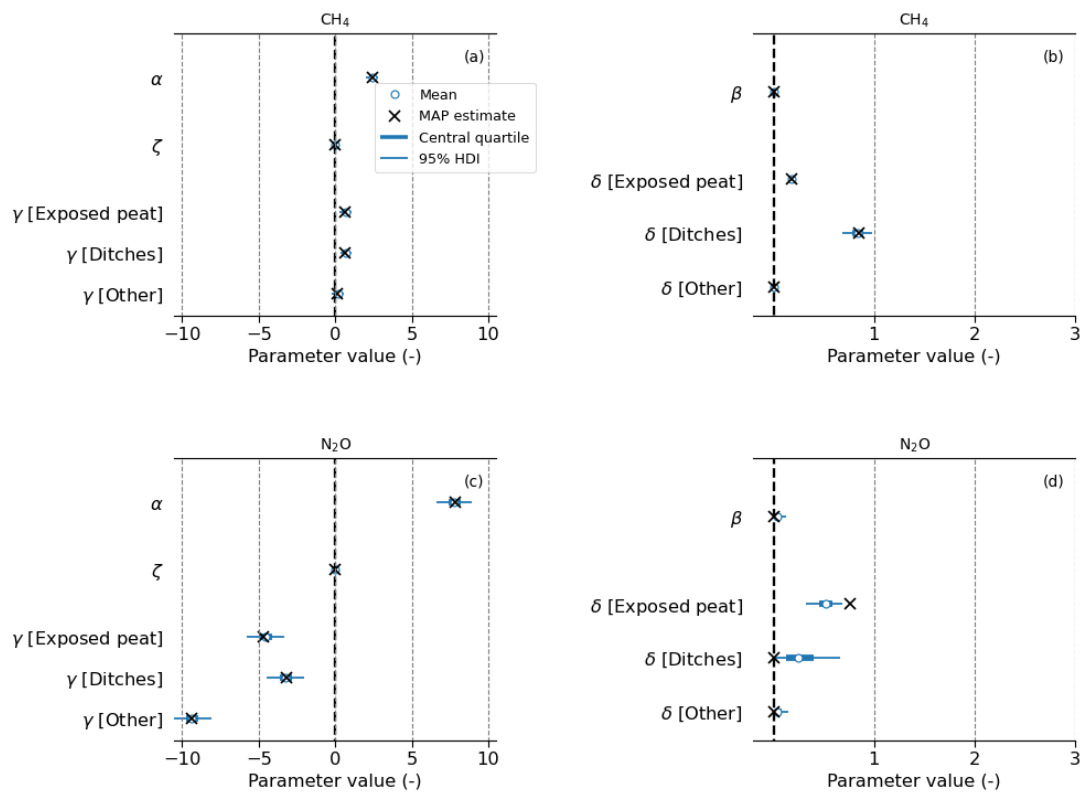


Figure S9: 95% highest posterior density interval for parameters of the full θ ST3 model for CH_4 (a-b) and N_2O (c-d). The bold line indicates the 25th and 75th percentiles of the distributions, white circles are the distribution means and black crosses show the maximum a posteriori (MAP) estimate.

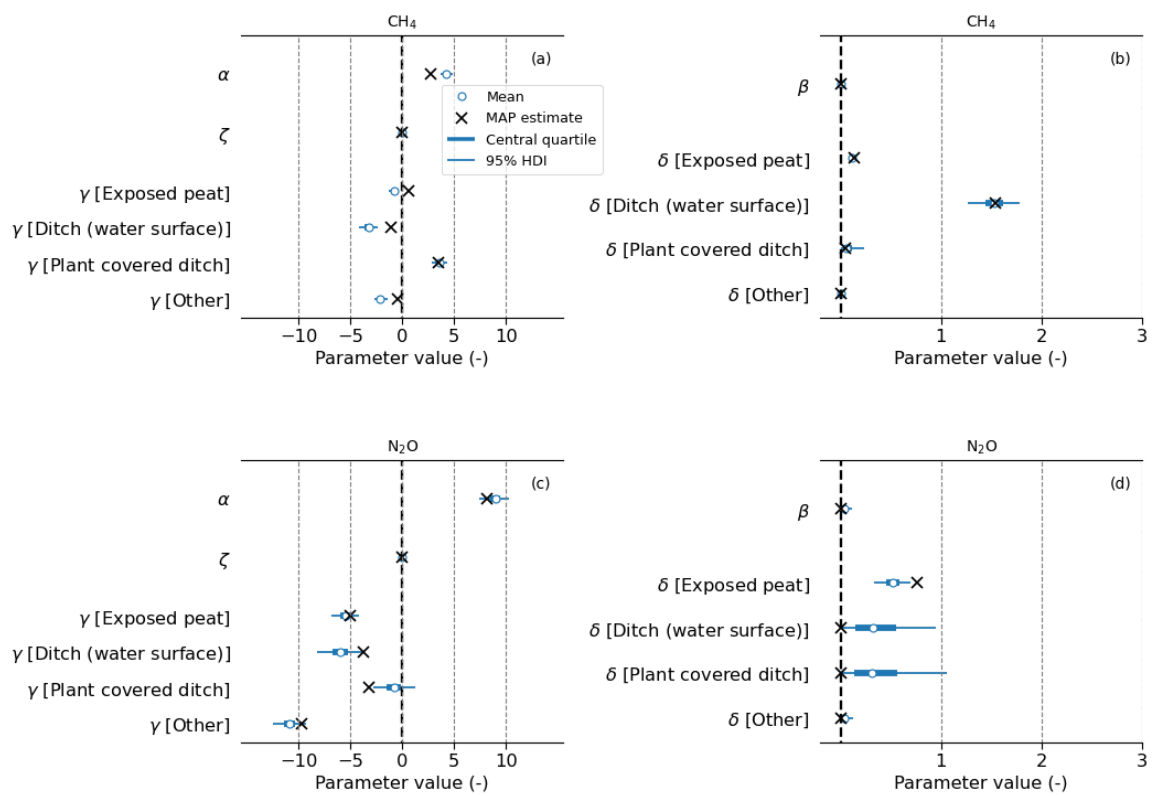


Figure S10: 95% highest posterior density interval for parameters of the full θ ST4 model for CH_4 (a-b) and N_2O (c-d). The bold line indicates the 25th and 75th percentiles of the distributions, white circles are the distribution means and black crosses show the maximum a posteriori (MAP) estimate.

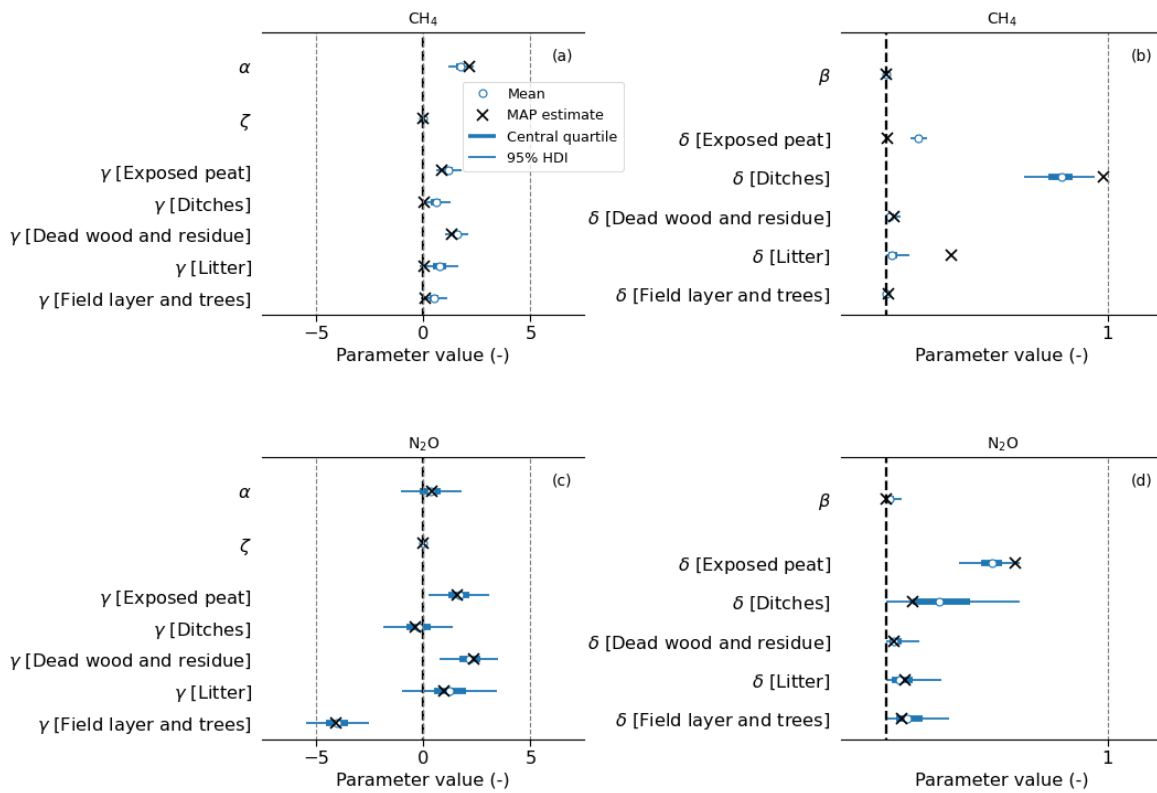


Figure S11: 95% highest posterior density interval for parameters of the full θ ST5 model for CH_4 (a-b) and N_2O (c-d). The bold line indicates the 25th and 75th percentiles of the distributions, white circles are the distribution means and black crosses show the maximum a posteriori (MAP) estimate.

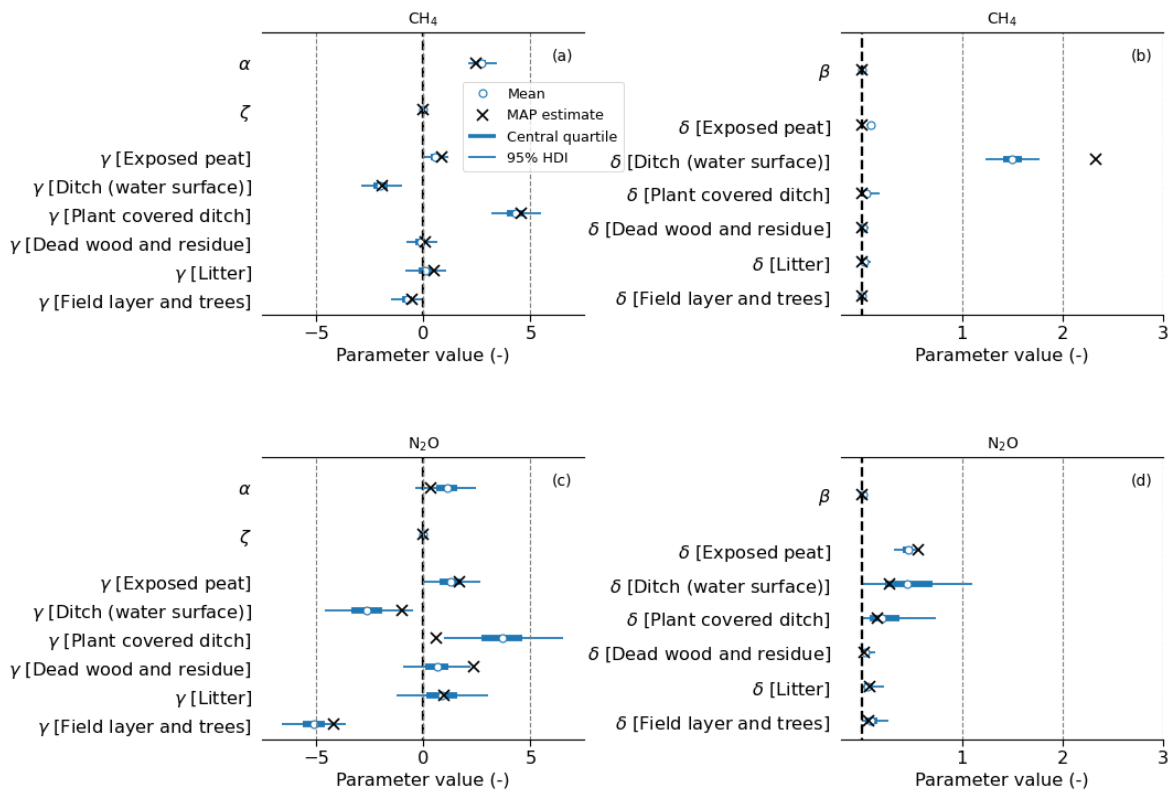


Figure S12: 95% highest posterior density interval for parameters of the full θ ST6 model for CH_4 (a-b) and N_2O (c-d). The bold line indicates the 25th and 75th percentiles of the distributions, white circles are the distribution means and black crosses show the maximum a posteriori (MAP) estimate.

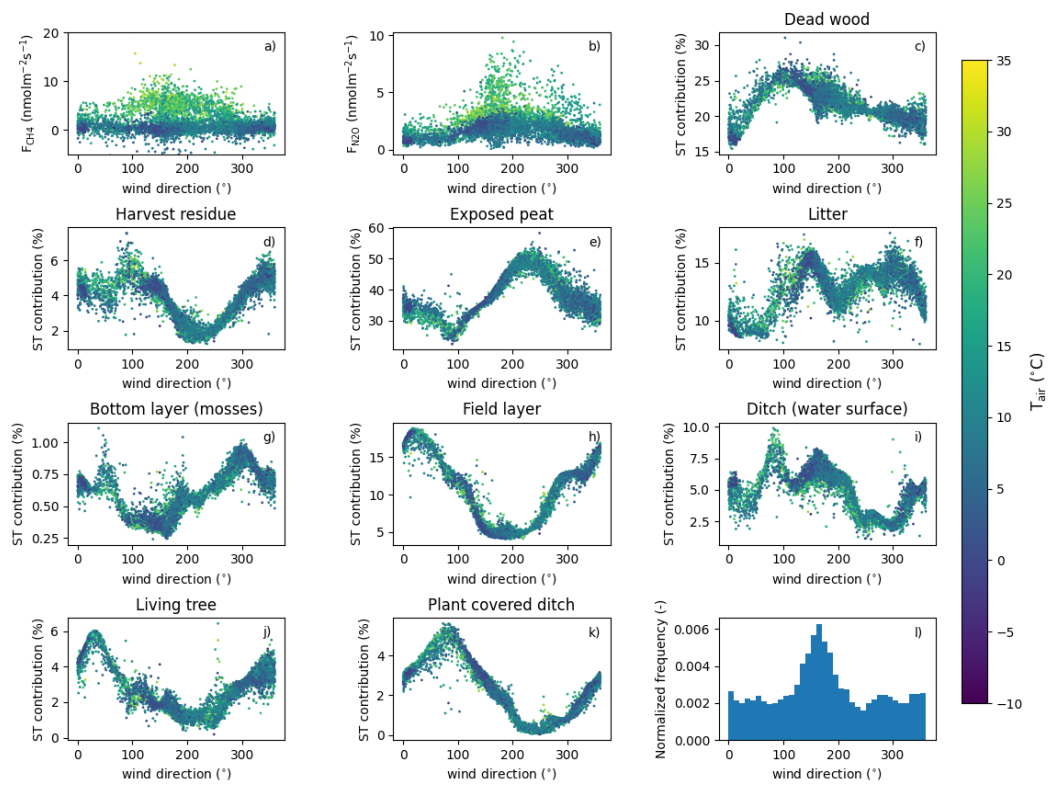


Figure S13. Analysis of wind direction dependencies. Wind direction dependency of CH₄ (a) and N₂O (b) fluxes, each surface-type contribution inside the eddy covariance footprint (c-k), and distribution of footprint wind directions (k). Color in panels a-k shows the air temperature.